OPTIMIZATION OF NANOFLUID-COOLED MICROCHANNEL HEAT SINK

by

Ahmed Mohammed ADHAM [a*], Normah Mohd-GHAZALI [b], and Robiah AHMAD [c]

[a] Refrigeration and Air Conditioning Engineering Techniques, Erbil Technical Engineering College, Erbil Polytechnic University, Erbil, Iraqi Kurdistan, Iraq
[b] Faculty of Mechanical Engineering, University of Technology Malaysia, Skudai, Johor Barhru, Malaysia
[c] UTM Razak School of Engineering and Advanced Technology, University of Technology Skudai, Johor Barhru, Malaysia International Campus, Jalan Semarak, Kuala Lumpur, Malaysia

Original scientific paper
DOI: 10.2298/TSCI130517163A

The optimization of a nanofluid-cooled rectangular microchannel heat sink is reported. Two nanofluids with volume fraction of 1%, 3%, 5%, 7%, and 9% are employed to enhance the overall performance of the system. An optimization scheme is applied consisting of a systematic thermal resistance model as an analysis method and the elitist non-dominated sorting genetic algorithm. The optimized results showed that the increase in the particles volume fraction results in a decrease in the total thermal resistance and an increase in the pumping power. For volume fractions of 1%, 3%, 5%, 7%, and 9%, the thermal resistances were 0.072, 0.07151, 0.07075, 0.07024, and 0.070 K/W for the SiC-H_2O while, they were 0.0705, 0.0697, 0.0694, 0.0692, and 0.069 K/W for the TiO_2-H_2O. The associated pumping power were 0.633, 0.638, 0.704, 0.757, and 0.807 W for the SiC-H_2O while they were 0.645, 0.675, 0.724, 0.755, and 0.798 W for the TiO_2-H_2O. In addition, for the same operating conditions, the nanofluid-cooled system outperformed the water-cooled system in terms of the total thermal resistance (0.069 and 0.11 for nanofluid-cooled, and water-cooled systems, respectively). Based on the results observed in this study, nanofluids should be considered as the future coolant for electronic devices cooling systems.

Key words: *microchannel, nanofluid, optimization, non-dominated sorting genetic algorithm*

Introduction

Since the landmark experiments by Tuckerman and Pease [1], microchannel heat sink (MCHS) has been established as an effective heat removal system in electronic chip packaging. The cooling system consists of parallel microchannels positioned atop the chip with a covering adiabatic plate to confine the coolant within. The fluid removes the heat as it flows through the channels. However, the rapid increase in the power density in inverse proportion to the size of the modern electronic chips has escalated intensive and extensive research into the cooling sys-

* Corresponding author; e-mail: ahamedadhm@yahoo.com, ahamed.adhm@epu.edu.krd.

tems of the MCHS. Areas investigated include the geometry, coolants, flow regimes, and materials [2-14].

The structural materials have so far reached its saturation stage with no new materials introduced that can replace the standard silicon and copper that cover the base silicon chip material. Coolants used in the past had been generally air and water due to their availability, working in any flow conditions, laminar and turbulent. Air has limited heat transfer capabilities while water requires a higher pumping power as well as posing a potential risk to the system damage at the slightest leakage. Ammonia has lately been proven to be good environmentally friendly coolant in the refrigeration and MCHS systems [15, 16]. With recent development in the nanotechnology, nanofluids have been introduced as an alternative coolant. The nanofluid generally consists of a base fluid such as water, oil and glycol to name a few, with the dispersion of nanosized particles made of metals, oxides, nitrides, or nanotubes. The inclusion of these nanoparticles changes the properties of the base fluid depending on the concentration of the particles [17]. Due to the increased in thermal conductivities of these nanofluids with the presence of the additional particles, heat transfer enhancements have been reported [18-21].

Lee and Mudawar [21] experimentally determined the effectiveness of alumina water based nanofluid in a MCHS. They found that the use of nanoparticles has significantly improved the overall performance when it was used in single phase flow compared to two-phase flow. Based on their observations, they discussed the suitability of using nanofluids as future coolants for microchannel heat sinks. Chein and Huang [22] in their analytical study with different volume fractions and channel configurations found that the overall performance of their rectangular microchannel system had significantly improved with a CuO-H_2O cooled rectangular MCHS. Numerical simulation by Mohammed *et al.* [23] on Al_2O_3-H_2O with various particle volume fractions (1-5%) of nanofluid indicated that the lowest thermal resistance for a rectangular MCHS was obtained for a volume fraction of 5%. They used a hybrid scheme finite-volume-method to model the performance of the laminar flow nanofluid coolant. Meanwhile, Li and Kleinstreuer [24] modeled their CuO-H_2O cooled trapezoidal microchannel heat sink using the entropy generation minimization method (EGM) for two particle volume fractions (1% and 4%) in the laminar flow region. They discovered that there exists an optimum Reynolds number range where the performance of MCHS is optimized. Escher *et al*. [25] developed a new Nusselt number correlation experimentally based on the different volume fractions of aqueous SiO_2-H_2O nanofluid (5%, 16%, and 31%) used in a rectangular MCHS. They stated that a better performance could be achieved with the increase in the specific heat capacity compared to the increased in thermal conductivity. In addition, they stated that based on the recorded data, the conventional Nusselt number correlation can be used to determine the heat transfer coefficient of nanofluid systems. In a recent publication, Ijam and Saidur [26] theoretically studied the overall performance of a rectangular minichannel heat sink cooled by SiC-H_2O and TiO_2-H_2O under a turbulent flow condition. Volume fractions of 0.8%, 1.6%, 2.4%, 3.2%, and 4% were used to determine the thermo-physical properties of the nanofluids. The overall results showed that for the 4% volume fraction, TiO_2-H_2O outperformed SiC-H_2O for a slightly higher pumping power demand. In general, the studies discussed in previous paragraphs presented parametric studies and performance examination of different nanofluids used as coolants which involves only flow conditions and volume fractions. Geometrical optimized dimensions and materials effect were not considered. They studied the effects of the nanoparticles volume fractions on the overall performance of their associated systems. This study reports the optimization of a rectangular microchannel heat sink using SiC-H_2O and TiO_2-H_2O nanofluids. Using the optimization scheme developed by Ahmed *et al.* [15] which is comprised of a thermal resistance and pressure

drop analysis models, and the non-dominated sorting genetic algorithm (NSGA-II) as an optimization algorithm, the overall performance is optimized under different particles volume fractions. The effects of the channel aspect ratio, the channel wall to channel width ratio and the use of different structural materials on the thermal resistance and the pumping power are presented too.

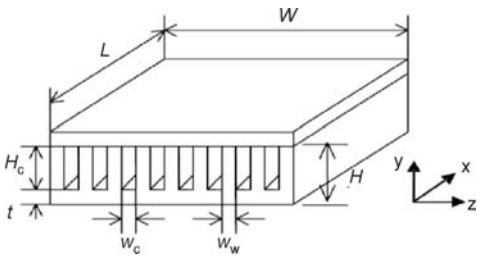

Figure 1. Schematic drawing of the microchannel heat sink model (adopted from [15])

Theory

The rectangular microchannel heat considered for the current analysis is depicted in fig. 1.

Two different nanofluids namely SiC-H_2O and TiO_2-H_2O [26] with volume fraction of 1%, 3%, 5%, 7%, and 9% are employed with their thermo-physical properties calculated based on the equations [27-30]:

$$\rho_{\mathrm{nf}} = (1+\phi)\rho_{\mathrm{f}} + \phi\rho_{\mathrm{p}} \tag{1}$$

$$\mu_{\mathrm{nf}} = \frac{1}{(1-\phi)^{2.5}}\mu_{\mathrm{f}} \tag{2}$$

$$(\rho Cp)_{\mathrm{nf}} = (1-\phi)(\rho Cp)_{\mathrm{f}} + \phi(\rho Cp)_{\mathrm{p}} \tag{3}$$

$$k_{\mathrm{nf}} = \frac{k_{\mathrm{p}} + (n-1)k_{\mathrm{f}} - (n-1)\phi(k_{\mathrm{f}} - k_{\mathrm{p}})}{k_{\mathrm{p}} + (n-1)k_{\mathrm{f}} + \phi(k_{\mathrm{f}} - k_{\mathrm{p}})}k_{\mathrm{f}} \tag{4}$$

The thermo-physical properties at 35 °C of the base fluid (water) and the nanoparticles used in the current study are taken from Lienhard *et al*. [31] and listed in tab. 1. The spherical particles are assumed for the nanoparticles with $n = 3$. In the current analysis, the dimensions and the operating conditions employed by Tuckerman and Pease [1] are utilized and tabulated in tab. 2. To facilitate the analysis the following assumptions are made:

– the flow was considered to be laminar steady flow,
– the coolant was an incompressible fluid,
– the interior walls of the channel were smooth, and
– the thermo-physical properties were assumed to be constant.

Table 1. Thermo-physical properties of the base fluid and nanoparticles at 35 °C

Thermo-physical properties	H_2O	SiC	TiO_2
Density, ρ [kgm^{-3}]	994.2	3160	4157
Specific heat capacity, Cp [Jkg^{-1}°K^{-1}]	4178	675	710
Thermal conductivity, k [Wm^{-1}°K^{-1}]	0.625	490	8.4
Viscosity, μ [Ns^{-1}m^{-2}]	$7.25\cdot10^{-4}$	–	–

Table 2. Geometrical parameters and operating conditions employed in the current study

Parameters	Values
Heat sink width, W [m]	$1\cdot10^{-2}$
Heat sink length, L [m]	$1\cdot10^{-2}$
Channel height, H_c [m]	$320\cdot10^{-6}$
Substrate thickness, t [m]	$213\cdot10^{-6}$
Volumetric flow rate, G [m^{3}s^{-1}]	$4.7\cdot10^{-6}$

In the current analysis, the thermal performance of the system is evaluated optimized using the thermal resistance equation given in [15]:

$$R_{\text{total}} = \frac{L}{Cp_{\text{nf}}\mu_{\text{nf}}} \frac{2}{\text{Re}} \frac{1+\beta}{1+\alpha} + \frac{1}{h_{\text{av}}} \frac{1+\beta}{1+2\alpha\eta} + \frac{t}{k_{\text{hs}}} \tag{5}$$

The hydrodynamic performance is assessed and optimized using the pressure drop/pumping power equation [15]:

$$\Delta p_{\text{tot}} = f_{\text{hs}} \frac{(1+\alpha)L}{2H_{\text{c}}} \rho_{\text{nf}} \frac{V_{\text{mnf}}^2}{2} + \left[1.79 - 2.23\left(\frac{1}{1+\beta}\right) + 0.53\left(\frac{1}{1+\beta}\right)^2\right] \rho_{\text{nf}} \frac{V_{\text{mnf}}^2}{2} \tag{6}$$

$$P_p = \Delta p_{\text{tot}}\, G \tag{7}$$

Equations (5), (6), and (7) contained two design variable namely, the channel aspect ratio ($\alpha = H_c/w_c$) and the wall width to channel width ratio ($\beta = w_w/w_c$) which are directly related to the rectangular microchannel geometry and will be used in the optimization process.

The average convective heat transfer coefficient appears in eq. (5) is evaluated using the following correlation proposed by Kim and Kim [32] for pure water flowing inside a rectangular microchannel:

$$h_{\text{av}} = 2.253 + 8.164\left(\frac{\alpha}{\alpha+1}\right)^{3/2} \frac{k_{\text{nf}}}{D_{\text{h}}} \tag{8}$$

The friction factor used in the calculation of the total pressure drop and consequently the pumping power is evaluated using the correlation formulated by Copeland [33] which considers the developing and the fully developed flow conditions and it has the form:

$$f\,\text{Re} = \left\{\left[3.2\left(\frac{\text{Re}\,D_{\text{h}}}{L}\right)^{0.57}\right]^2 + (4.7 + 19.64B)^2\right\}^{1/2} \tag{9}$$

$$B = \frac{\left(\frac{1}{\alpha}\right)^2 + 1}{\left(\frac{1}{\alpha} + 1\right)^2} \tag{10}$$

Optimization procedure

In the current study, the system is treated as a multi-objective functions system with two objective functions related to its thermal and hydrodynamic performances. The first objective function is the total thermal resistance, eq. (5), while the second is the pumping power, eq. (7). The NSGA-II is invoked to optimize (minimize) both objective functions simultaneously. The design variables (α and β) limits are listed in tab. 3. The same optimization procedure employed in [15] is followed and modified in order to generate a Pareto optimal front with obvious trade-off between both objective functions. The modification was in terms of the employed cross-over function in which the arithmetic function was used instead of the scattered function used in [15]. In addition, the uniform

Table 3. Design variables limits

Limits	Design variables	
	α	β
Upper	10	0.1
Lower	1	0.01

function was used as a mutation function. These modifications significantly enhanced the generated Pareto optimal front in which denser front in terms of the number of the optimal solutions compared to the one generated in [15] is observed. Lastly, the complete optimization procedure employed in the current study is illustrated in fig. 2.

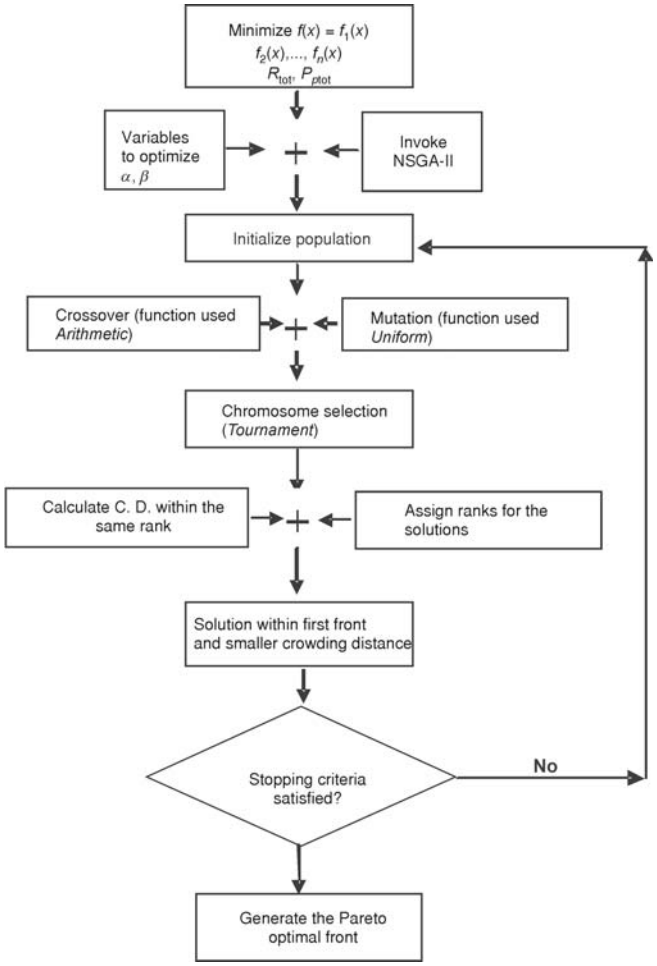

Figure 2. The complete optimization procedure for the current study (adopted from [15])

Results and discussion

Effect of the particle volume fraction (ϕ)

The effect of the particle volume fraction on the thermal resistance and pumping power is studied for volume fractions of 1%, 3%, 5%, 7%, and 9% for both nanofluids, the SiC-H_2O and TiO_2-H_2O. Table 4 lists the nanofluids thermo-physical properties used in the current study. Figure 3 shows the effect of the particle volume fraction on the total thermal resistance. It can clearly be seen that the thermal resistance is decreasing with the increase in the volume fraction. A previous study [26] showed that the increased nanoparticles volume fraction increased the thermal conductivity of the coolant. The increase in the thermal conductivity actually increases the convective heat transfer coefficient which in turn reduces the convective thermal resistance and consequently the total thermal resistance. The lowest thermal resistance is achieved with the

Table 4. Nanofluid thermo-physical properties used in the current study

Properties	SiC-H_2O					TiO_2-H_2O				
	1%	3%	5%	7%	9%	1%	3%	5%	7%	9%
ρ_{nf} [kgm^{-3}]	1020	1060	1100	1150	1190	1030	1090	1150	1021	1280
$\mu_{nf}\cdot10^{-4}$ [Nsm^{-3}]	7.43	7.82	8.23	8.69	9.17	7.43	7.82	8.23	8.69	9.17
Cp_{nf} [Jkg^{-1}K^{-1}]	4070	3860	3670	3500	3340	4040	3780	3550	3340	3161
k_{nf} [Wm^{-1}K^{-1}]	0.644	0.683	0.723	0.765	0.809	0.64	0.67	0.703	0.736	0.771

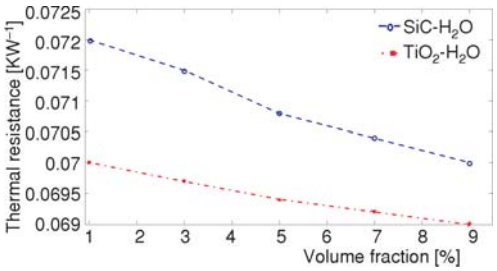

Figure 3. Effect of the volume fraction on the thermal resistance

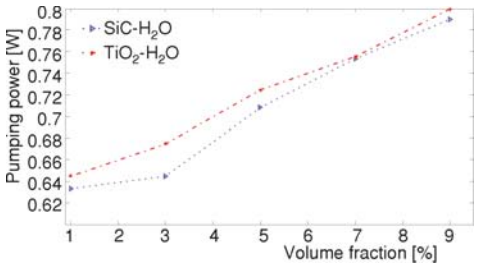

Figure 4. Effect of the volume fraction on the pumping power

volume fraction of 9%. Hence, this volume fraction is used to conduct a parametric study in the next section. Figure 4 depicts the effect of the nanoparticles volume fraction on the pumping power. The pumping power is increasing with the increase in the volume fraction. The increase in the volume fraction increases the density (tab. 4) which increases the total pressure drop of the system which ultimately increases the required pumping power to drive the coolant.

Effect of the geometric parameters (design variables)

The effects of the channel aspect ratio (α) on the thermal resistance and pumping power for volume fraction of 9% are illustrated in figs. 5 and 6. It can be seen that with the increase in the channel aspect ratio, the thermal resistance is decreasing while the pumping power is increasing. The increase in the aspect ratio can be attributed to a single reason which is the decrease in the channel width because the channel height is kept constant through the entire optimization process. The decrease in the channel width enhances the convective heat transfer coefficient [1] which reduces the convective thermal resistance. Knowing that the convective thermal resistance is the dominant term in the total thermal resistance therefore, its decrease reduces the total thermal resistance and this behavior explains what is illustrated in fig. 5. As for the pumping power, it is an established fact that the narrow channels require more pumping power to circulate the coolant. This confirms the behavior noticed in fig. 6 that shows an increase in the pumping power for the increase in the channel aspect ratio. The relation observed between the channel aspect ratio and the pumping power is compatible with the fact that the lowest thermal resistance is always accompanied with the highest pumping power.

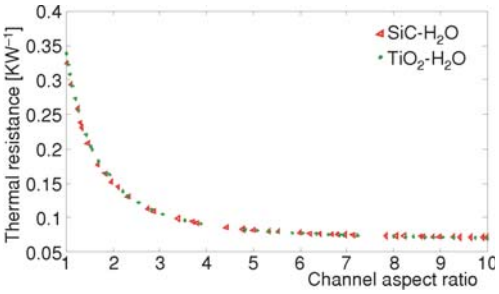

Figure 5. Effect of the channel aspect ratio on the thermal resistance

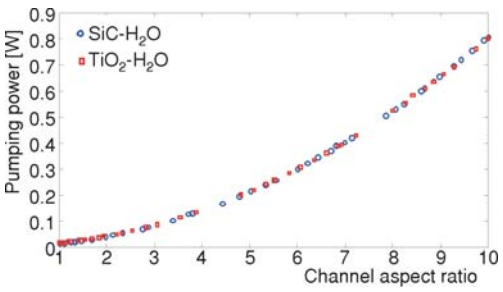

Figure 6. Effect of the channel aspect ratio on the pumping power

Figures 7 and 8 demonstrate the effects of the wall width to channel width ratio (β) on the thermal resistance and the pumping power. Similar behavior to the channel aspect ratio is observed in which the increase in the wall width to the channel width ratio leads to a decrease in the thermal resistance and an increase in the pumping power. Based on the definition of β, for a particular wall width, the increment is attributed to the decrease in the channel width. This behavior confirms the behavior noticed when the effect of the channel aspect ratio is studied in which the decrease in the thermal resistance and the increase in the pumping power were attributed to the decrease in the channel width. In general, it can be inferred that the system performance is more sensitive to α than β. The effect of α on the thermal resistance and pumping power was evenly distributed along the entire range of the α limits (tab. 3) while it was only sparsely distributed for the small range of β values allowed in tab. 3.

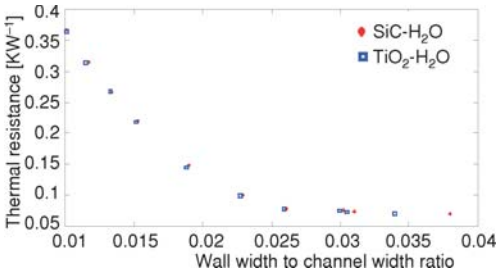

Figure 7. Effect of the wall width to channel width ration on the thermal resistance

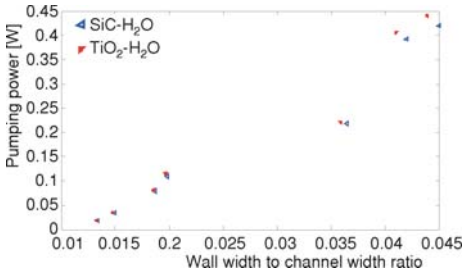

Figure 8. Effect of the wall width to channel width ration on the pumping power

Effect of the structural material

The effect of using different structural materials on the overall performance of the system is depicted in figs. 9 and 10. Three materials namely, silicon, aluminum, and copper were used and their thermal conductivity values are 148, 238, and 400 W/mK], respectively. No significant difference in the thermal resistance is observed between the two nanofluids investigated with the various structural materials. When SiC-H_2O was used, the lowest achievable thermal resistances were 0.0705, 0.066, and 0.063 K/W for silicon, aluminum, and copper, respectively. The thermal resistance values were 0.069, 0.065, and 0.062 K/W for silicon, aluminum, and copper when TiO_2-H_2O was used as a coolant. In both cases, however, copper was superior to aluminum and silicon. Table 5 summarizes the optimized results for the three different materials.

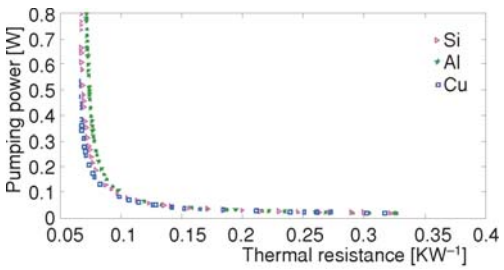

Figure 9. Effect of different structural material on the system's performance when SiC-H_2O is used

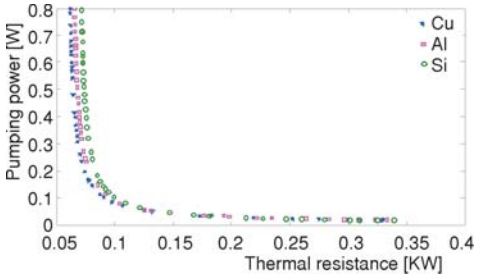

Figure 10. Effect of different structural materials on the system's performance when TiO_2-H_2O is used

Table 5. Optimized results for different structural materials

Coolant	Optimized results	Material		
		Si	Al	Cu
SiC-H_2O	R [KW^{-1}]	0.0705	0.066	0.063
	P_p [W]	0.797	0.798	0.798
	α	9.999	9.998	9.994
	β	0.01	0.011	0.012
TiO_2-H_2O	R [KW^{-1}]	0.069	0.065	0.062
	P_p [W]	0.796	0.8	0.799
	α	9.993	9.996	9.990
	β	0.01	0.014	0.015

The overall performance noticed in figs. 9 and 10 encourages the use of higher thermal conductivity materials to fabricate the microchannel heat sink. The use of higher thermal conductivity material reduces the thermal resistance significantly from two aspects. The first aspect is that higher thermal conductive material reduces the conductive thermal resistance through the substrate. The second aspect is that the higher thermal conductivity material enhances the wall efficiency to transfer the heat into the coolant *i. e.* reduces the convective thermal resistance. In general, if better performance is desired regardless of the resulting component weight, then, higher thermal conductive materials should be utilized.

Conclusions

In the current study, the performance optimization of a microchannel heat sink is conducted using two nanofluids. Several conclusions were made.

- The thermal resistance and the pumping power were significantly affected by the variation in the nanoparticles volume fraction. With the increase in the volume fraction, the thermal resistance is decreasing while the pumping power is increasing.
- For the same operating conditions employed by Tuckerman and Pease [1] for pure water, SiC-H_2O and TiO_2-H_2O provided lower thermal resistance compared to pure water (0.0705, 0.069, and 0.11 for SiC-H_2O, TiO_2-H_2O, and water, respectively.
- The overall performance of TiO_2-H_2O was better than SiC-H_2O in terms of the thermal resistance and the pumping power. For the volume fraction of 9%, the thermal resistance and pumping power of TiO_2-H_2O were 0.069 K/W and 0.798 W compared to 0.07 K/W and 0.807 W for SiC-H_2O. Although, the gain is under 2%, this advantage is appreciable considering that this is for only a 1 cm × 1 cm heat sink.
- The performance of the system was more responsive with the variation in the channel aspect ratio than the wall width to channel width ratio. This requires precise fabrication process of the microchannel heat sink.
- Higher thermal conductive materials are recommended for the microchannel heat sink which uses nanofluids as coolants. Aluminum can be used because it provides a balance between the high heat removal capabilities and the preferred light weight desired in microchannel systems.

Nomenclature

Cp – specific heat, [Jkg^{-1}K^{-1}]
D_h – hydraulic diameter, [m]
f – friction factor
G – volumetric flow rate, [m^{3}s^{-1}]
H – heat sink height, [m]
H_c – channel height, [m]
h_{av} – heat transfer coefficient, [Wm^{-2}K^{-1}]
k – thermal conductivity, [Wm^{-1}K^{-1}]
L – heat sink length, [m]
n – spherical particle parameter
P_p – pumping power, [W]
Δp – pressure drop, [kPa]
R – thermal resistance, [KW^{-1}]
Re – Reynolds number
t – substrate thickness, [m]
W – heat sink width, [m]
w_c – channel width, [μm]

w_w – wall (fin) width, [μm]
V_{mf} – velocity inside the microchannel, [ms^{-1}]

Greek symbols

α – channel aspect ratio
β – wall width to channel width ratio
η – fin efficiency
μ – viscosity, [kgs^{-1}m^{-1}]
ρ – density, [kgm^{-3}]
ϕ – particle volume fraction, [%]

Subscripts

c – channel
f – fluid (coolant)
nf – nanofluid
hs – heat sink
p – particle
w – wall

References

[1] Tuckerman, D. B., Pease, R. F. W., High Performance Heat Sinking for VLSI, *IEEE Electr DEV Lett, 2* (1981), 5, pp. 126-129
[2] Hetsroni, G., *et al*., Drag Reduction and Heat Transfer of Surfactants Flowing in a Capillary Tube, *International Journal of Heat and Mass Transfer, 47* (2004), 17-18, pp. 3797-3809
[3] Tiselj, I., *et al*., Effect of Axial Conduction on the Heat Transfer in Micro-Channels, *International Journal of Heat and Mass Transfer, 47* (2004), 12-13, pp. 2551-2565
[4] Kleiner, M. B., *et al.*, High Performance Forced Air Cooling Scheme Employing Microchannel Heat Exchangers, *IEEE Transaction, Components*, *Hybrids and Manufacturing Technology-part A., 18* (1995), 4, pp. 795-804
[5] Wen, Z., Choo, F. K., The Optimum Thermal Design of Microchannel Heat Sinks, IEEE/CPMT, *Proceedings,* 1th Electronic Packaging Technology Conference, Singapur, 1997, pp. 123-129
[6] McHale, J. P., Garimella, S. V., Heat Transfer in Trapezoidal Microchannels of Various Aspect Ratios, *International Journal of Heat and Mass Transfer, 53* (2010), 1-3, pp. 365-375
[7] Perret, C., *et al*., Microchannel Integrated Heat Sinks in Silicon Technology, *Proceedings*, 1998 IEEE Industry Applications Conference, St. Louis, Mo., USA, 1998, (2), pp. 1051-1055
[8] Hetsroni, G., *et al*., Heat Transfer in Micro-Channels: Comparison of Experiments with Theory and Numerical Results, I*nternational Journal of Heat and Mass Transfer, 48* (2005), 25-26, pp. 5580-5601
[9] Khan, W. A., *et al*., Optimization of Microchannel Heat Sinks Using Entropy Generation Minimization Method, *IEEE Transaction on Components and Packaging Technologies, 32* (2009), 2, pp. 243-251
[10] Liu, D., Garimella, S. V., Analysis and Optimization of the Thermal Performance of Microchannel Heat Sinks, *International Journal for Numerical Methods in Heat and Fluid Flow, 15* (2005), 1, pp. 7-26
[11] Goldberg, N., Narrow Channel Forced Air Heat Sink, *IEEE Transaction, Components, Hybrids, and Manufacturing Technology, CHMT-7* (1984), 1, pp. 154-159
[12] Kosar, A., Effect of Substrate Thickness and Material on Heat Transfer in Microchannel Heat Sinks, *International Journal of Thermal Sciences, 49* (2010), 4, pp. 635-642
[13] Liu, K. V., *et al*., Measurements of Pressure Drop and Heat Transfer in Turbulent Pipe Flows of Particulate Slurries, Report, Argonne National Laboratory, Lemont, Ill., USA, 1988, ANL-88-15
[14] Ahmed, M. A., *et al*., Thermal and Hydrodynamic Analysis of Microchannel Heat Sinks: *A Review, Renewable and Sustainable Energy Reviews, 21* (2013), May, pp. 614-622
[15] Ahmed, M. A., *et al.*, Optimization of an Ammonia-Cooled Rectangular Microchannel Heat Sink Using Multi-Objective Non-Dominated Sorting Genetic Algorithm (NSGA2), *Heat and Mass Transfer, 48* (2012), 10, pp. 1723-1733
[16] Pamitran, A. S., *et al*., Nasrudin, Evaporation Heat Transfer Coefficient in Single Circular Small Tubes Flow Natural Refrigerants of C_3H_8, NH_3, and CO_2, *Int. J. of Multiphase Flow, 37* (2011), 7, pp. 794-801
[17] Hung, T. C., *et al*., Heat Transfer Enhancement in Microchannel Heat Sinks Using Nanofluids, *International Journal of Heat and Mass Transfer, 55* (2012), 9-10, pp. 2559-2570
[18] Byrne, M. D., *et al*., Experimental Thermal-Hydraulic Evaluation of CuO Nanofluids in Microchannels at Various Concentrations with and without Suspension Enhancers, *International Journal of Heat and Mass Transfer, 55* (2012), 9-10, pp. 2684-2691
[19] Ho, C. J., *et al*., An Experimental Investigation of Forced Convective Cooling Performance of a Microchannel Heat Sink with Al_2O_3/Water Nanofluid, *Applied Thermal Engineering, 30* (2010), 2-3, pp. 96-103
[20] Chein, R., Chuang, J., Experimental Microchannel Heat Sink Performance Studies using Nanofluids, *International Journal of Thermal Sciences, 46* (2007), 1, pp. 57-66

[21] Lee, J., Mudawar, I., Assessment of the Effectiveness of Nanofluids for Single-Phase and Two-Phase Heat Transfer in Micro-Channels, *Int. J. Heat Mass Transfer, 50* (2007), 3-4, pp. 452-463
[22] Chein, R., Huang, G., Analysis of Microchannel Heat Sink Performance Using Nanfluids, *Applied Thermal Engineering, 25* (2005), 17-18, pp. 3104-3114
[23] Mohammed, H. A., *et al*., Heat Transfer in Rectangular Microchannels Heat Sink Using Nanofluids, *International Communication in Heat and Mass Transfer, 37* (2010), 10, pp. 1496-1503
[24] Li, J., Kleinstreuer, C., Entropy Generation Analysis for Nanofluid Flow in Microchannels, *Journal of Heat Transfer, 132* (2011), 12, pp. 122401-1-122041-8
[25] Escher, W., *et al*., On the Cooling of Electronics with Nanofluids, *Journal of Heat Transfer, 133* (2011), May, pp. 051401-1-051401-11
[26] Ijam, A., Saidur, R., Nanofluid as a Coolant for Electronic Devices (Cooling of Electronic Devices), *Applied Thermal Engineering, 32* (2012), Jan., pp. 76-82
[27] Drew, D. A., Passman, S. L., *Theory of Multicomponents Fluids*, Springer, Berlin, 1999
[28] Brinkman, H. C., The Viscosity of Concentrated Suspensions and Solutions, *Journal of Chemical Physics, 20* (1952), 4, pp. 571-581
[29] Yang, S. M., Tao, W. Q., *Heat Transfer*, 3rd ed., Higher Education Press, Beijing, China, 1998
[30] Hamilton, R. L., Crosser, O. K., Thermal Conductivity of Heterogeneous Two-Components Systems, *Industrial and Engineering Chemistry Fundamentals, 1* (1962), 3, pp. 182-191
[31] Lienhard, I. V., *et al*., *Heat Transfer Textbook*, 3rd ed., Phlogiston Press, Cambridge Massachusetts, USA, 2008
[32] Kim, S. J., Kim, D., Forced Convection in Microstructures for Electronic Equipment Cooling, *Journal of Heat Transfer, 121* (1999), 3, pp. 639-645
[33] Copeland, D., Optimization of Parallel Plate Heat Sinks for Forced Convection, 16th IEEE Semi-therm Symposium, San Jose, Cal., USA, 2000, pp. 266-272

Paper submitted: May 17, 2013
Paper revised: August 8, 2013
Paper accepted: October 13, 2013